A comparative study of the interaction of *Bartonella henselae* strains with human endothelial cells

Chao-Chin Chang[a], Ya-Jou Chen[b], Chih-Sian Tseng[b], Wan-Ling Lai[b], Kai-Yang Hsu[b], Chao-Liang Chang[b], Chi-Cheng Lu[c] and Yuan-Man Hsu[b,*]

[a]Graduate Institute of Microbiology and Public Health, School of Veterinary Medicine, National Chung Hsing University, Taichung 402, Taiwan

[b]Department of Biological Science and Technology, College of Life Sciences, China Medical University, Taichung 404, Taiwan

[c]Department of Life Sciences, College of Life Sciences, National Chung Hsing University, Taichung 402, Taiwan

Running title: A comparative study of *Bartonella henselae* strains

[*]Corresponding Author: Yuan-Man Hsu
China Medical University
91, Hsueh-Shih Road, Taichung, Taiwan
Tel: +886-4-22053366 ext 2503
Fax: +886-4-22071507
E-mail: yuanmh@mail.cmu.edu.tw

Abstract

Bartonella henselae can cause a wide range of clinical outcomes and may lead to severe disease, especially in patients with acquired immunodeficiency syndrome. It is well-known that *B. henselae*-induced cell proliferation is mediated by anti-apoptotic activity; however, the detailed mechanism is still unclear. In this study, the cellular responses of endothelial cells after infection with four *B. henselae* strains were compared and protein candidates that may be involved in the interaction between cells and bacteria were determined. The Houston-1 strain elicited the fastest response in terms of stimulating endothelial cell proliferation, and the JK-40 strain had the strongest ability to induce cell proliferation. By Western blot analysis, it was demonstrated that *B. henselae*-induced cell proliferation involved the mitochondria intrinsic apoptotic pathway. In addition, the adhesion abilities of the U-4 and JK-40 strains were much greater than those of the Houston-1 and JK-47 strains; however, the ability of Houston-1 to invade host cells was high. By two-dimension gel electrophoresis analysis, it was found that succinyl-CoA synthetase subunit beta, phage-related protein, and ATP synthase subunit alpha might be involved in the invasion process. The expression of superoxide dismutase [Cu-Zn] precursor increased with infection time for all four strains but was significantly higher in the Houston-1 strain, which may increase the competitive advantage of Houston-1 in terms of survival in host cells and render it successful in invading host cells and stimulating cell proliferation. Our data suggest that the interaction of *B. henselae* and endothelial cells differed between strains, and the results indicated possible candidate proteins that may play a role in the pathogenesis of *B. henselae* infection.

Keywords: *Bartonella henselae*, cellular responses, mitochondria intrinsic apoptotic pathway.

1. Introduction

Bartonella henselae is a facultative intracellular bacterium that is capable of causing a variety of syndromes. The most common *B. henselae*-associated disease is self-limited cat-scratch disease; however, life-threatening bacillary angiomatosis and bacillary peliosis also occur in humans (Anderson and Neuman, 1997). Domestic cats are the main reservoir for *B. henselae*, which is transmitted from cat to cat via the cat flea, with 5– 80% of cats testing seropositive, indicating previous exposure (Boulouis et al., 2005; Dehio, 2004).

Two genotypes/serotypes of *B. henselae* (types I and II) have been identified by 16S rRNA gene sequencing (Bergmans et al., 1996; Drancourt et al., 1996; La Scola et al., 2002). By epidemiological study, great diversity in the distribution of *B. henselae* infection in cats and humans of different geographical origin has been found (Boulouis et al., 2005). One previous report suggested that *B. henselae* 16S rRNA genotype I infection was more likely to be associated with vascular proliferative lesions of the liver and/or spleen and 16S rRNA genotype II with infection of the skin and/or lymph nodes (Chang et al., 2002). Nevertheless, the contributions of the above differences between type I and type II to *B. henselae* virulence are still unknown.

In vitro studies have shown that *Bartonella*-triggered vasoproliferation results in cell invasion, endothelial cell proliferation, and the inhibition of endothelial cell apoptosis (Dehio, 2004). Therefore, in this study, we compared the abilities of four *B. henselae* strains, including two strains of 16S rRNA genotype I and two strains of genotype II, to invade host cells and stimulate endothelial cell proliferation. The protein profiles of these four strains were also analyzed by two-dimensional electrophoresis (2-DE). It was demonstrated that the interaction of *B. henselae* and endothelial cells differed between strains, and the results provided possible candidate proteins that may play a role in the pathogenesis of *B. henselae* infection.

2. Materials and methods

2.1. Bacterial strains and cell culture

The *B. henselae* strains used in this study were Houston-1 (ATCC 49882) and U-4, provided by Professor Bruno B. Chomel (University of California, Davis, USA), and JK-47 and JK-40, which were gifts from Professor Jane E. Koehler (University of California, San Francisco, USA), as detailed in Table 1. Bacteria were grown on chocolate agar and maintained at 37°C in a 5% CO_2 incubator. Human microvascular endothelial cell line-1 (HMEC-1) (Lin et al., 2002) cells were passaged in culture plates containing endothelial cell growth medium composed of 2% fetal bovine serum (FBS), 1 μg ml^{-1} hydrocortisone, 10 ng ml^{-1} epidermal growth factor, and antibiotics (100 U ml^{-1} of penicillin and 100 μg ml^{-1} of streptomycin) (Lin et al., 2005). Cells were detached using 1000 U ml^{-1} trypsin and 0.5 mM ethylenediaminetetraacetate (EDTA), and only those cultures from three to five passages found to have a viability of >95% by eosin Y staining were used for experiment.

2.2. Proliferation assay

HMEC-1 cells were seeded onto 96-well plates at a density of 1×10^4 cells/well and were infected with bacteria at multiplicities of infection (MOIs) of 50 and 100 for 24, 48 and 72 h. The trypan blue exclusion protocol was used to determine cell viability. Briefly, a total of 10 μl of cell suspension in phosphate-buffered saline (PBS, pH 7.4) was mixed with 40 μl of trypan blue, and the numbers of stained (dead cells) and unstained cells (live cells) were counted using a hemacytometer. All assays were replicated three times and the proliferation activity was calculated as the relative change in comparison with the control groups (uninfected cells).

2.3. Western blot analysis

Following treatment of cells for 48h at a MOI of 50, 1×10^4 cells were collected and lysed in lysis buffer (0.5 M Tris-HCl, pH 7.4, 10% SDS, 0.5 M DTT). After incubation for 5min and boiling for 5min, whole cell lysates were collected by centrifugation at 10,000×g for 10 min, and a total of 10 µg of whole cell lysates was separated by sodium dodecyl sulphate (SDS) – polyacrylamide gel electrophoresis (PAGE) using a Hoefer mini VE system. Protein was then transferred to a PVDF membrane according to the manufacturer's instructions, and following transfer, the membrane was washed with PBS and blocked for 1 h at 37°C with 5% fat free milk in TBS and 0.1% of Tween 20 (TBST). The primary antibody (β-actin [Chemicon, USA], Bad [Cell Signaling, USA], cytochrome *c*, caspase 3, caspase 9 [BioLegend, USA], or Bcl-xL [Santa Cruz, USA]) was added at a dilution of 1/1000, following which blots were incubated at 37°C for 1 h with the peroxidase-conjugated secondary antibodies (goat anti-mouse IgG and goat anti-rabbit IgG, purchased from Santa Cruz Biotechnology) at a dilution of 1/20,000. Following removal of the secondary antibody, blots were washed with TBST twice and developed by Immobilon Western chemiluminescent HRP substrate (Millpore, USA), and the densities of the spots on the resulting immunoblots were quantified using a FUJIFILM LAS-3000.

2.4. Adherence and invasion assays

B. henselae adherence to and invasion of HMEC-1 cells were assessed as previously described with minor modifications (Kempf et al., 2001). Prior to infection with *B. henselae*, HMEC-1 cells were washed three times with culture medium without antibiotics. Cells were then seeded into 96-well flat-bottom plates at 1×10^4 cells per well and incubated overnight at 37°C, following which the bacteria were

added at a MOI of 50 or 100. To test the association ability of *B. henselae*, cells were processed at 48 h and 72 h to remove the culture supernatant, washed extensively with culture medium, and subjected to osmotic lysis to calculate the total number of bacteria (Kempf et al., 2001), including adhered and invaded bacteria. The number of viable *Bartonellae* was determined by quantitative plating of serial dilutions of the lysates on chocolate agar plates. Plates were cultured in candle jars at 37°C for 7 days, and the colonies were then counted. To perform the invasion assays, the infected cell culture supernatants were removed gently, cells were washed extensively with culture medium, and gentamicin (100 µg ml^{-1}) was added for 2 h to kill extracellular bacteria. Cells were then washed extensively to remove gentamicin, and osmotic lysis was performed as described above. The number of adhered bacteria was calculated by subtracting the number of bacteria that had invaded into the cells from the number associated with the cells, and the adherence/invasion rates were estimated by dividing the number of adhered/invaded bacteria by the number of HMEC-1 cells.

2.5. Two dimensional-gel electrophoresis

B. henselae was sonicated on ice using a microtip with the power level set between 4 and 5 at 20% duty, with a 10-sec short burst followed by a 10-sec interval for 20 min. The total proteins were precipitated using 10% trichloroacetic acid (TCA) and proteins were separated by two dimensional-gel electrophoresis (2-DE) as follows. The protein sample (600µg) was loaded onto 18-cm Readystrip IPG strips (Amersham Biosciences, UK) in the pH range of 3–10NL (nonlinear) and layered with 0.8 ml cover oil to prevent the gel from drying or urea crystallization. The gel was then run on an Ettan IPGPhor II (Amersham Biosciences, UK) at 30 V to rehydrate the gel strip for 16 h, followed by the running programs 500 V for 1 h with 500 Vh, 1000 V for 1 h with 1000 Vh, and 8000 V for 8 h with 64000 Vh. The voltage ramped

automatically based on the increasing resistance of the strip as excess ions moved out of the strip. After the first-dimension IEF, the strip was washed to remove the cover oil and then equilibrated in 5 ml of equilibration buffer containing 50 mM Tris-HCl, pH 8.8, 6 M urea, 2% SDS, 30% glycerol, and 1% DTT for 12~15 min. The strip was then subjected to a second equilibration, with 5 ml equilibration buffer with 1.5% iodoacetamide substituted for the DTT, for an additional 12~15 min. Next, SDS-PAGE was run using a PROTEAN II xi cell tank (Bio-Rad, USA) at 200 V for 4 h. Following electrophoresis, the gel was stained with 0.25% (w/v) coomassie R-250 (Amersham Biosciences, UK), and spots with differential expression levels between strains were selected manually and digested by trypsin for subsequent matrix-assisted laser desorption ionization (MALDI) time of flight (TOF)/TOF analysis. Mass spectrometry (MS) and protein identification were performed by the Mission Biotech Co., Ltd., Taiwan. Tandem MS was performed on a QSTARXL (Applied Biosystems-Sciex, Ontario, Canada) hybrid quadropole-time-of-flight mass spectrometer. Mascot software (Matrix Sciences Inc., Beachwood, OH, USA) was used to identify proteins from the NCBInr protein database of the National Center for Biotechnology Information at the National Institutes of Health.

2.6. Preparation of RNA and real-time PCR analysis

Total RNAs were extracted from cells or bacteria with TRIzol reagent and the amount of RNA estimated by spectrophotometry at 260nm. For real-time (RT)-PCR analysis, two-step RT-PCR was carried out using a high-capacity cDNA reverse transcription kit (Applied Biosystems, USA), and a 16S rRNA gene PCR assay was used as a housekeeping gene control assay. The reactions were performed in 20 µl (total volume) mixtures containing primers at a concentration of 400 nM. The reaction conditions consisted of 2 min at 50°C, 10 min at 95°C, then 40 cycles of 15 s at 95°C,

followed by 1 min at 60°C. Melting curve analysis was used to determine the PCR specificity and was performed using 80 10-s cycles, with the first cycle at 60°C and the temperature increasing by 0.5°C for each succeeding cycle. All reactions were carried out in triplicate from three independent bacterial cultures. Each assay was run on an Applied Biosystems 7300 Real-Time PCR system. The threshold cycle (Ct) is defined as the fractional cycle number at which the fluorescence passes the fixed threshold data, and was determined using the default threshold settings. Relative quantification of mRNA expression was calculated using the $2^{-\Delta\Delta Ct}$ method (Applied Biosystems User Bulletin N°2 (P/N 4303859)). Data were presented as the relative expression of target mRNA, normalized with respect to 16s RNA and relative to a calibrator sample that was collected at 0 h of infection. The primers used in this study are shown in Table 3.

2.7. DNA sequencing

In order to verify the differences between strains, the genes encoding those proteins identified by 2-DE were sequenced. Primers were designed based on the published sequence of the *B. henselae* Houston-1 genome (GenBank accession No. BX897699). All of the primer sequences used for PCR amplification are listed in Table 4. PCR was performed in a total volume of 25 µl, which contained 5 µl of supernatant, 20 pmol of each primer, 1.25 U of Taq Plus DNA polymerase, 1.75 mM $MgCl_2$, and 200 µM dNTP (PCR Master Mix Kit, Genemark). After an initial denaturation step of 2 min at 95°C, the primer mix was amplified for 35 cycles, each consisting of 1 min at 95°C, 1 min at the hybridization temperature of 50°C, and 1 min at 72°C, with a final extension step of 15 min at 72°C. Primers and free nucleotides were removed using a PCR Clean-Up Kit (Genemark). Both strands of the PCR products were sequenced using AmpliTaq-FS DNA polymerase and dye

terminator chemistry at the DNA sequencing facility at Mission Biotech Co., Ltd., Taiwan. The oligonucleotide primers were synthesized by the same company. The nucleotide sequences were analyzed using the BLAST program (National Center for Biotechnology Information (NCBI), U.S. National Library of Medicine)(Altschul and Koonin, 1998; Altschul et al., 1997).

2.8. Statistical analysis

The data were analyzed using SPSS version 10 (SPSS Inc., Chicago, IL, USA). The difference between mean values among groups was first evaluated by one-way analysis of variance (ANOVA) and then pairwise comparison of the mean values between the two groups, followed by Tukey's Student Rank test. Differences with a *P* value < 0.05 were considered significant.

3. RESULTS

3.1. Different B. henselae *strains possess differing abilities to induce cell proliferation.*

The cell viabilities after 48 h of infection with the Houston-1 strain at MOIs of 50 and 100 were significantly higher than those after infection with other strains (p<0.05)(Fig. 1), and Houston-1 strain infection resulted in a 1.33-fold increase in cell numbers as compared with uninfected controls at 48 h at MOIs of both 50 and 100. However, infection with the JK-40 strain resulted in a 1.74-fold increase in cell proliferation at a MOI of 50, but this was observed at 72 h. The U-4 strain also induced a 1.48-fold increase at 72 h but at a MOI of 100. Overall, the Houston-1 strain exhibited the fastest response in terms of stimulating HMEC-1 cell proliferation, and the JK-40 strain had the strongest ability to induce cell proliferation. Infection

with the JK-47 strain did not significantly affect the cell viability of HMEC-1 cells.

3.2. The anti-apoptotic activity of B. henselae *is mediated via the mitochondria intrinsic apoptotic pathway*

We further examined the pathway involved in this phenomenon and compared the anti-apoptotic activity between strains. As shown in Fig. 2, the expressions of Bad, Bcl-xl, cytochrome *c*, caspase 9, and caspase 3 were monitored. Compared with U-4- and JK-47-infected cells, Houston-1 and JK-40 infection did not induce expression of the apoptotic proteins Bad, cytochrome *c*, caspase 9, or caspase 3; however, expression of the anti-apoptotic protein Bcl-xl was up-regulated in Houston-1-infected cells but down-regulated in JK-47-infected cells. Houston-1 infection did not significantly affect the apoptotic protein expression, but increased the expression of Bcl-xl. Furthermore, U-4 and JK-47 infection increased the expression of apoptotic proteins in HMEC-1 cells, and JK-47 also caused down-regulation of Bcl-xl. The pathway involved in the release of pro-apoptotic proteins and active caspase enzymes from mitochondria is the mitochondria intrinsic apoptotic pathway. Our results indicated that U-4 and JK-47 infection triggered the mitochondria intrinsic apoptotic pathway. Nevertheless, Houston-1 infection induced the expression of anti-apoptotic protein Bcl-xl, which inhibited cytochrome *c* release from mitochondria and led to cell proliferation. Therefore, Houston-1-mediated anti-apoptotic activity also involved the intrinsic pathway.

3.3. The adherence and invasion abilities differed between B. henselae *strains.*

We further evaluated the abilities of the different *B. henselae* strains to adhere to and invade host cells (Fig. 3). U-4 and JK-40 possessed strong abilities to adhere to HMEC-1 cells at MOIs of 50 and 100 at 48 h and 72 h: at 48 h, the adherence rates of

these two strains was positively proportional to the MOI, while at 72 h, the adherence rates were decreased; this was also true for the JK-47 strain. The best adherence rate was achieved at 48 h for the U-4 (67.6 CFU/cell), JK-47 (18.1 CFU/cell), and JK-40 (43.9 CFU/cell) strains; however, the Houston-1 strain had a relatively low ability to become adherent to host cells. Comparing the invasion abilities of the strains, the Houston-1 strain exhibited the best ability to invade host cells in a dose- and time-dependent manner.

3.4. Proteomic analysis of B. henselae *strains*

To identify differences in bacterial proteins between the *B. henselae* strains, proteomic analysis of all four strains was performed. The proteins that differed are candidate proteins for involvement in the different phenotypes. We compared the protein profiles of the Houston-1 and U-4 strains (Fig. 4A) and those of the JK-47 and JK-40 strains (Fig. 4B). A total of 246 and 226 protein spots were detected by 2-DE analysis of Houston-1 and U-4, respectively, with a match percentage of 88.55% (209 spots) between strains, while a total of 337 and 330 protein spots were detected by 2-DE analysis of JK-47 and JK-40, respectively, with a match percentage of 97.75% (326 spots) between strains.

Those proteins for which at least a 2-fold difference in protein expression between strains was detected were followed up by protein determination and infection culture. Two proteins (BH-D and BH-E) with higher expression levels in the Houston-1 strain than in the U-4 strain were identified by 2-DE analysis; the expression levels of three other proteins (BU-A, BU-B, and BU-C) were higher in the U-4 strain specifically. Six other proteins were also identified by 2-DE analysis, their expression levels being higher in either JK-47 (47-A, 47-B, and 47-D) or JK-40 (40-C, 40-E, and 40-F). These 11 spots were subjected to MALDI-TOF/TOF MS

determination of proteins (results shown in Table 2).

The RNA expression levels of superoxide dismutase [Cu-Zn] precursor (BH-D), succinyl-CoA synthetase subunit beta (BU-A), phage-related protein (BU-B), ATP synthase subunit alpha (47-A), and small heat-shock protein (40-E) in the bacteria were found to be correlated with the 2-DE analysis results; therefore, the RNA expression levels of these 5 proteins were further analyzed after *in vitro* infection of endothelial cells at a MOI of 50 for 24, 48, and 72h (Fig. 5). Superoxide dismutase [Cu-Zn] precursor was expressed in all strains, and its expression increased with infection time, the highest expression being observed in the Houston-1 strain and the lowest in the JK-47 strain (Fig. 5A). Succinyl-CoA synthetase subunit beta and ATP synthase subunit alpha were expressed most highly in the Houston-1 strain at 24 and 48 h, respectively (Fig. 5B and Fig. 5E), and phage-related protein was markedly up-regulated in the Houston-1 strain at 48 h after infection, its expression in JK-47 also being significantly increased at 72 h of infection (Fig. 5C). Small heat-shock protein was expressed most highly in the JK-47 strain at 72 h of infection; however, the Houston-1 strain elicited the fastest response in terms of expressing small heat-shock protein (at 48 h of infection) (Fig. 5D).

The RNA expression level of BadA was monitored after *in vitro* infection of endothelial cells (Fig. 5F), and all four strains were found to express BadA, which was up-regulated at 24 h in the U-4 strain and at 48 h in the Houston-1 and JK-40 strains.

4. DISCUSSION

In this study, we compared the interaction between *B. henselae* strains and endothelial cells, and also determined the protein candidates that may be involved in

B. henselae infection. Furthermore, this study demonstrated that *B. henselae* infection involves the mitochondria intrinsic apoptotic pathway.

Among the *B. henselae* strains compared in this study, the Houston-1 strain possessed the fastest ability to stimulate cell proliferation and suppress the mitochondria-mediated apoptotic pathway overall; nevertheless, the U-4 and JK-40 strains also exhibited similar abilities after a 24-hour delay. In endothelial cells, *B. henselae* is known to induce cell proliferation via an anti-apoptotic pathway, and several studies have shown that caspase activation and DNA fragmentation are involved (Dehio, 2003; Kempf et al., 2005; Kempf et al., 2001; Kirby and Nekorchuk, 2002; Schmid et al., 2006; Schmid et al., 2004). However, these studies did not investigate other proteins associated with the apoptotic pathway. In this study, we demonstrated that *B. henselae* infection involves the mitochondria intrinsic pathway, and U-4 and JK-47 infection mediated the intrinsic apoptotic pathway. As shown in previous studies (Adams and Cory, 1998; Green and Reed, 1998; Gross et al., 1999), in the mitochondria intrinsic pathway, the binding of the pro-apoptotic regulator Bad inhibits the anti-apoptotic protein Bcl-2/Bcl-xl, thereby releasing cytochrome *c* and activating the caspase cascade. In contrast with the U-4 and JK-47 strains, Houston-1 infection decreased Bad expression but increased the level of Bcl-xl, which prevented the release of cytochrome *c* from mitochondria and activation of the caspase cascade. As the U-4 strain was able to induce cell proliferation at 72 h after infection, there must be another mechanism that strongly affects cell proliferation.

In this study, the association abilities of the strains were further analyzed and compared, and the adhesion abilities of U-4 and JK-40 were found to be much greater than those of Houston-1 and JK-47. The Houston-1 strain did not tend to adhere to the surface of endothelial cells, but U-4, JK-47, and JK-40 reached a plateau of adherence to endothelial cells at 48 h of infection. Houston-1 had a strong ability to invade

endothelial cells, and this strain also stimulated cell proliferation remarkably. Although the mechanism is still unknown, it is reasonable to hypothesize that the strain with the better ability to invade cells might possess a better ability to stimulate cell proliferation, as observed with the Houston-1 strain. Even though the U-4 and JK-40 strains did not tend to invade cells, they were able to induce endothelial cell proliferation, but with a 24-h delay; thus, an unknown mechanism might be involved in cell proliferation induced by infection.

The number of spots in our 2-DE analysis is different from what have been reported (Eberhardt et al., 2009; Zhao et al., 2005). Using a smaller strips (18cm IPG strips) and a relatively insensitive staining method (coomassie blue staining) cause less detectable spots in our 2-DE study. 2-DE analysis may still provide useful information for characterization of the virulence of *B. henselae* strains. The match percentage between the Houston-1 and U-4 strains was 88.5%, which is much lower than that between the Houston-1 and Marseille strains (95%) (Zhao et al., 2005); however, the match percentage was 97.75% between the JK-47 and JK-40 strains, and therefore there was no consistency between 16s rRNA genotype and protein profile.

Superoxide dismutase [Cu-Zn] precursor, succinyl-CoA synthetase subunit beta, phage-related protein, ATP synthase subunit alpha, and small heat-shock protein were identified by 2-DE analysis and the protein profiles of the different strains compared, variation in which may result in differences in bacteria–cell interaction between strains. The immunodominant seromarkers in the Marseille strain have been identified by 2-DE analysis (Eberhardt et al., 2009) to be dihydrolipoamide succinyltransferase, the protein GI 49475876, the elongation factor Tu, chaperonin protein groEL, the elongation factor Ts, and parvulin-like peptidyl-prolyl *cis-trans* isomerase – these immunodominant proteins are quite different from the proteins we identified in this study. Thus, the proteins responsible for bacteria–cell interaction might differ from the

immunoreactive proteins.

RT-PCR was applied to monitor the expression of specific genes, and 16s rRNA was used as an internal control in our study. It has been reported that the interaction of *B. henselae* and endothelial cells causes rapid bacterial rRNA synthesis within the first 18 h of infection (Kempf et al., 2000); however, in our infection system, there was no significant difference in 16s rRNA synthesis between strains from 24 h to 72 h after infection. This inconsistency between the results of previous studies and the findings of this study may reflect differences in the *B. henselae* strains and the MOIs used for infection; therefore, 16s rRNA was still used as an internal control in our study.

By RT-PCR analysis, succinyl-CoA synthetase subunit beta, phage-related protein, and ATP synthase subunit alpha were found to be highly-expressed in the Houston-1 strain after just 24 h of infection. Succinyl-CoA synthetase is an essential enzyme that catalyzes the carboxylation of fatty acid biosynthesis, and thus bacteria need this enzyme for membrane lipid biogenesis and growth (Liu et al., 2008). By sequence analysis, phage-related protein has been found to be a DNA single-strand annealing protein involved in DNA recombination pathways. Homologous DNA recombination is a fundamental process in the biochemistry of DNA repair and replication, and contributes to the generation of genetic diversity critical for natural selection (Kuzminov, 2001). ATP synthase subunit alpha is an enzyme that generates energy and is essential for bacterial survival (Greie et al., 2000). It has not been demonstrated that any of these proteins are involved of the pathogenesis of *Bartonellae* infection; however, our data indicated that they might play a role in the ability of Houston-1 to stimulate cell proliferation and invasion. The expression patterns of small heat-shock protein observed in the different *B. henselae* strains were approximately correlated with their abilities to stimulate cell proliferation. Small heat-shock protein is a chaperone and can protect misfolded proteins against

irreversible aggregation (Kuczynska-Wisnik et al., 2004); it is also an immunogenic protein (Haake et al., 1997; Young, 1990). The chaperonin protein groEL, chaperonin protein groES, heat-shock protein 70 Dnak, Hsp-70 cofactor grpE, and the small heat-shock protein IpbA2 are able to react with *B. henselae* immune serum (Eberhardt et al., 2009); therefore, small heat-shock protein may play an important role in cell proliferation after *B. henselae* infection. Superoxide dismutase (SOD) could protect cells from the toxic effects of reactive oxygen species, and as shown previously, SOD contributes to the survival of *Salmonella* Typhimurium in macrophages (Craig and Slauch, 2009). The expression of superoxide dismutase [Cu-Zn] precursor in *B. henselae* increased with duration of infection and was significantly higher in the Houston-1 strain than in the other strains examined. Expression of SOD increases the competitive advantage of bacterial survival in host cells. Houston-1 has the ability to exist in endothelial cells, and demonstrated the best ability to invade host cells.

In conclusion, this is the first study to demonstrate that *B. henselae*-induced cell proliferation involves the mitochondria intrinsic apoptotic pathway. In addition, the results indicated that the Houston-1 strain exhibits the fastest response in terms of stimulating HMEC-1 cell proliferation and the best ability to invade host cells, while the U-4 and JK-40 strains have strong abilities to induce cell proliferation and adhere to endothelial cells. The bacterial proteins superoxide dismutase [Cu-Zn] precursor, succinyl-CoA synthetase subunit beta, phage-related protein, ATP synthase subunit alpha, and small heat-shock protein identified by proteomic analysis might play important roles in the pathogenesis of *B. henselae*, and further study of these proteins is therefore required .

Acknowledgments

This investigation was supported by research grants from the National Science Council (NSC93-2313-B-039-004) and China Medical University (CMU93-ST-02, CMU94-033 and CMU95-031).

References

Adams, J.M., Cory, S., 1998, The Bcl-2 protein family: arbiters of cell survival. Science 281, 1322-1326.

Altschul, S.F., Koonin, E.V., 1998, Iterated profile searches with PSI-BLAST--a tool for discovery in protein databases. Trends Biochem Sci 23, 444-447.

Altschul, S.F., Madden, T.L., Schaffer, A.A., Zhang, J., Zhang, Z., Miller, W., Lipman, D.J., 1997, Gapped BLAST and PSI-BLAST: a new generation of protein database search programs. Nucleic Acids Res 25, 3389-3402.

Anderson, B.E., Neuman, M.A., 1997, Bartonella spp. as emerging human pathogens. Clin Microbiol Rev 10, 203-219.

Bergmans, A.M., Schellekens, J.F., van Embden, J.D., Schouls, L.M., 1996, Predominance of two Bartonella henselae variants among cat-scratch disease patients in the Netherlands. J Clin Microbiol 34, 254-260.

Boulouis, H.J., Chang, C.C., Henn, J.B., Kasten, R.W., Chomel, B.B., 2005, Factors associated with the rapid emergence of zoonotic Bartonella infections. Vet Res 36, 383-410.

Chang, C.C., Chomel, B.B., Kasten, R.W., Tappero, J.W., Sanchez, M.A., Koehler, J.E., 2002, Molecular Epidemiology of Bartonella henselae Infection in Human Immunodeficiency Virus-Infected Patients and Their Cat Contacts, Using Pulsed-Field Gel Electrophoresis and Genotyping. J Infect Dis 186, 1733-1739.

Craig, M., Slauch, J.M., 2009, Phagocytic superoxide specifically damages an extracytoplasmic target to inhibit or kill Salmonella. PLoS ONE 4, e4975.

Dehio, C., 2003, Recent progress in understanding Bartonella-induced vascular proliferation. Curr Opin Microbiol 6, 61-65.

Dehio, C., 2004, Molecular and cellular basis of bartonella pathogenesis. Annu Rev Microbiol 58, 365-390.

Drancourt, M., Birtles, R., Chaumentin, G., Vandenesch, F., Etienne, J., Raoult, D., 1996, New serotype of Bartonella henselae in endocarditis and cat-scratch disease. Lancet 347, 441-443.

Eberhardt, C., Engelmann, S., Kusch, H., Albrecht, D., Hecker, M., Autenrieth, I.B., Kempf, V.A., 2009, Proteomic analysis of the bacterial pathogen Bartonella

henselae and identification of immunogenic proteins for serodiagnosis. Proteomics 9, 1967-1981.

Green, D.R., Reed, J.C., 1998, Mitochondria and apoptosis. Science 281, 1309-1312.

Greie, J.C., Deckers-Hebestreit, G., Altendorf, K., 2000, Subunit organization of the stator part of the F0 complex from Escherichia coli ATP synthase. Journal of bioenergetics and biomembranes 32, 357-364.

Gross, A., McDonnell, J.M., Korsmeyer, S.J., 1999, BCL-2 family members and the mitochondria in apoptosis. Genes Dev 13, 1899-1911.

Haake, D.A., Summers, T.A., McCoy, A.M., Schwartzman, W., 1997, Heat shock response and groEL sequence of Bartonella henselae and Bartonella quintana. Microbiology 143 (Pt 8), 2807-2815.

Kempf, V.A., Schairer, A., Neumann, D., Grassl, G.A., Lauber, K., Lebiedziejewski, M., Schaller, M., Kyme, P., Wesselborg, S., Autenrieth, I.B., 2005, Bartonella henselae inhibits apoptosis in Mono Mac 6 cells. Cell Microbiol 7, 91-104.

Kempf, V.A., Schaller, M., Behrendt, S., Volkmann, B., Aepfelbacher, M., Cakman, I., Autenrieth, I.B., 2000, Interaction of Bartonella henselae with endothelial cells results in rapid bacterial rRNA synthesis and replication. Cell Microbiol 2, 431-441.

Kempf, V.A., Volkmann, B., Schaller, M., Sander, C.A., Alitalo, K., Riess, T., Autenrieth, I.B., 2001, Evidence of a leading role for VEGF in Bartonella henselae-induced endothelial cell proliferations. Cell Microbiol 3, 623-632.

Kirby, J.E., Nekorchuk, D.M., 2002, Bartonella-associated endothelial proliferation depends on inhibition of apoptosis. Proc Natl Acad Sci U S A 99, 4656-4661.

Kuczynska-Wisnik, D., Zurawa-Janicka, D., Narkiewicz, J., Kwiatkowska, J., Lipinska, B., Laskowska, E., 2004, Escherichia coli small heat shock proteins IbpA/B enhance activity of enzymes sequestered in inclusion bodies. Acta Biochim Pol 51, 925-931.

Kuzminov, A., 2001, DNA replication meets genetic exchange: chromosomal damage and its repair by homologous recombination. Proc Natl Acad Sci U S A 98, 8461-8468.

La Scola, B., Liang, Z., Zeaiter, Z., Houpikian, P., Grimont, P.A., Raoult, D., 2002, Genotypic characteristics of two serotypes of Bartonella henselae. J Clin Microbiol 40, 2002-2008.

Lin, C.F., Chiu, S.C., Hsiao, Y.L., Wan, S.W., Lei, H.Y., Shiau, A.L., Liu, H.S., Yeh, T.M., Chen, S.H., Liu, C.C., Lin, Y.S., 2005, Expression of cytokine, chemokine, and adhesion molecules during endothelial cell activation induced by antibodies against dengue virus nonstructural protein 1. J Immunol 174, 395-403.

Lin, C.F., Lei, H.Y., Shiau, A.L., Liu, H.S., Yeh, T.M., Chen, S.H., Liu, C.C., Chiu, S.C., Lin, Y.S., 2002, Endothelial cell apoptosis induced by antibodies against dengue virus nonstructural protein 1 via production of nitric oxide. J Immunol 169, 657-664.

Liu, X., Fortin, P.D., Walsh, C.T., 2008, Andrimid producers encode an acetyl-CoA carboxyltransferase subunit resistant to the action of the antibiotic. Proc Natl Acad Sci U S A 105, 13321-13326.

Schmid, M.C., Scheidegger, F., Dehio, M., Balmelle-Devaux, N., Schulein, R., Guye, P., Chennakesava, C.S., Biedermann, B., Dehio, C., 2006, A translocated bacterial protein protects vascular endothelial cells from apoptosis. PLoS Pathog 2, e115.

Schmid, M.C., Schulein, R., Dehio, M., Denecker, G., Carena, I., Dehio, C., 2004, The VirB type IV secretion system of Bartonella henselae mediates invasion, proinflammatory activation and antiapoptotic protection of endothelial cells. Mol Microbiol 52, 81-92.

Young, D.B., 1990, Chaperonins and the immune response. Seminars in cell biology 1, 27-35.

Zhao, S.Q., Cai, Y.F., Zhu, Z.Y., 2005, Comparative proteomic analysis of B. henselae Houston and B. henselae Marseille by two-dimensional gel electrophoresis. Biomed Environ Sci 18, 341-344.

Figure legends

Fig. 1. Effects of *B. henselae* strains on stimulation of HMEC-1 cell proliferation. (A) MOI=50; (B) MOI=100. The numbers in parentheses indicate the 16S rRNA genotype. Results are presented as the mean of the relative fold change as compared with the control groups. *: significant difference ($p<0.05$) between strains at 48 h; #: significant difference ($p<0.05$) between strains at 72 h. The results are representative of three independent experiments carried out in triplicate. The error bars indicate standard deviation.

Fig. 2. Effect of *B. henselae* infection on the expression levels of Bad, Bcl-xl, cytochrome *c*, caspase 9 and caspase 3. *: significant difference ($p<0.05$) in comparison with the control groups (uninfected cells). (A) Western blot; (B) quantitative analysis of Western blot. The numbers in parentheses indicate the 16S rRNA genotype. All assays were replicated in three independent experiments. The error bars indicate standard deviation.

Fig. 3. Association abilities of the different *B. henselae* strains at MOIs of 50 and 100 after 48 and 72 h. (A) adherence rate; (B) invasion rate. The adherence/invasion rates were estimated by dividing the number of adhered/invaded bacteria by the number of HMEC-1 cells. The numbers in parentheses indicate the 16S rRNA genotype. All assays were replicated in three independent experiments. The error bars indicate standard deviation.

Fig. 4. 2-DE analysis of total proteins in (A) Houston-1 (16S rRNA genotype I, left) and U4 (16S rRNA genotype II, right); (B) JK47 (16S rRNA genotype I, left) and JK40 (16S rRNA genotype II, right).

Fig. 5. RNA expression levels of strain-specific proteins in different *B. henselae* strains after infection. (A) BH-D (superoxide dismutase [Cu-Zn] precursor); (B) BU-A (acetyl-CoA carboxylase carboxyltransferase subunit alpha); (C) BU-B (phage-related protein); (D) 47-A (ATP synthase subunit alpha); (E) 40-E (small heat-shock protein). Results are presented as relative fold in comparison with the U-4-infected groups. The numbers in parentheses indicate the 16S rRNA genotype. The results are representative of three independent experiments carried out in triplicate. The error bars indicate standard deviation.

Table 1. *B. henselae* strains used in this study.

Strain	Genotype	Origin	Reference
Houston-1	I	Blood of an HIV-positive patient	(Regnery et al., 1992)
U-4	II	Blood of a naturally-infected cat	(Abbott et al., 1997)
JK-47	I	HIV-infected patient who clinically exhibited bacteremia, BA lesions of the skin and lymph nodes, and BP lesions of the liver and spleen	(Werner et al., 2006)
JK-40	II	HIV-infected patient with only lymph node involvement	None

Table 2. MALDI-TOF/TOF MS spectral analysis of identified *B. henselae* proteins.

Spot	Accession No.	Protein Description	Theoretical Mr(Da)/pI
BH-D	gi|49475620	Superoxide dismutase [Cu-Zn] precursor	18850/5.87
BH-E	gi|49476039	Hypothetical protein BH13580	19684/6.14
BU-A	gi|49476285	Acetyl-CoA carboxylase carboxyltransferase subunit alpha	34927/6.28
BU-B	gi|49475174	Phage-related protein	29123/5.80
BU-C	gi|49475510	Small heat-shock protein	19074/5.56
47-A	gi|49476189	ATP synthase subunit alpha	55477/5.91
47-B	gi|49476305	Succinyl-CoA synthetase subunit beta	42790/5.07
47-D	gi|49474982	Inorganic pyrophosphatase	20015/5.13
40-C	gi|49475012	Peptidyl-prolyl cis-trans isomerase	35575/5.81
40-E	gi|49475510	Small heat-shock protein	19074/5.56
40-F	gi|49475510	Small heat-shock protein	19074/5.56

1 **Table 3.** Primers used for *B. henselae* RT-PCR.

Protein	**Primer**	**Sequence (5`-3`)**
Superoxide dismutase [Cu-Zn] precursor	BHD-F	GTGCCGCAGGTGGTCATTAT
	BHD-R	TCGACATACAGTGCTGGTAAGTCA
Acetyl-CoA carboxylase carboxyltransferase subunit alpha	BUA-F	GCCAGCCATAGCCTCTAAAGC
	BUA-R	CATTATTCCGGAGCCCTTAGG
Phage-related protein	BUB-F	GCATTTCCGCAGCAGATCA
	BUB-R	CGGCAAGATTGTTGACTTTGG
ATP synthase subunit alpha	47A-F	AGCACCGAGTCGTTTAACACAA
	47A-R	TGGTATGGCACTCAATTTGGAA
Small heat-shock protein	40E-F	GCGTTTTCATTTAGCTGATCATGTT
	40E-R	CGGCATTTCTCTTTTAAGCTGAAT
BadA	BadA-F	TTGATGCTGGCGTTAGAGGTT
	BadA-R	GCACCTACAGAGCTTTTCCATACA
16s rRNA	16S-F	GAGAAGAAGCCCCGGCTAAC
	16S-R	TATCCGCCTACATGCGCTTT

2

Table 4. Primers used for sequencing *B. henselae* genes.

Protein	**Primer**	**Sequence (5`-3`)**
Superoxide dismutase [Cu-Zn] precursor	BHD-SF	AATAATGGGTGTTTTTGTCG
	BHD-SR	AATTTCACCAGTTTGATTGG
Acetyl-CoA carboxylase carboxyltransferase subunit alpha	BUA-SF	GCTATCAGCACAAAAGATCC
	BUA-SR	TATCGTTTAGTCAATGAACATCA
Phage-related protein	BUB-SF	CCTATGCTAACAAAATCCTTATT
	BUB-SR	TCCTCTGTTAATCGCTCTGT
Small heat-shock protein	40E-SF	TGATGATGAAGGGTTAAGAA
	40E-SR	GAGCCATATACGAAACTTCA

Figure legends

Fig. 1. Effects of *B. henselae* strains on stimulation of HMEC-1 cell proliferation. (A) MOI=50; (B) MOI=100. The numbers in parentheses indicate the 16S rRNA genotype. Results are presented as the mean of the relative fold change as compared with the control groups. *: significant difference ($p<0.05$) between strains at 48 h; #: significant difference ($p<0.05$) between strains at 72 h. The results are representative of three independent experiments carried out in triplicate. The error bars indicate standard deviation.

Fig. 2. Effect of *B. henselae* infection on the expression levels of Bad, Bcl-xl, cytochrome *c*, caspase 9 and caspase 3. *: significant difference ($p<0.05$) in comparison with the control groups (uninfected cells). (A) Western blot; (B) quantitative analysis of Western blot. The numbers in parentheses indicate the 16S rRNA genotype. All assays were replicated in three independent experiments. The error bars indicate standard deviation.

Fig. 3. Association abilities of the different *B. henselae* strains at MOIs of 50 and 100 after 48 and 72 h. (A) adherence rate; (B) invasion rate. The adherence/invasion rates were estimated by dividing the number of adhered/invaded bacteria by the number of HMEC-1 cells. The numbers in parentheses indicate the 16S rRNA genotype. All assays were replicated in three independent experiments. The error bars indicate standard deviation.

Fig. 4. 2-DE analysis of total proteins in (A) Houston-1 (16S rRNA genotype I, left) and U4 (16S rRNA genotype II, right); (B) JK47 (16S rRNA genotype I, left) and JK40 (16S rRNA genotype II, right).

Fig. 5. RNA expression levels of strain-specific proteins in different *B. henselae* strains after infection. (A) BH-D (superoxide dismutase [Cu-Zn] precursor); (B) BU-A (acetyl-CoA carboxylase carboxyltransferase subunit alpha); (C) BU-B (phage-related protein); (D) 47-A (ATP synthase subunit alpha); (E) 40-E (small heat-shock protein). Results are presented as relative fold in comparison with the U-4-infected groups. The numbers in parentheses indicate the 16S rRNA genotype. The results are representative of three independent experiments carried out in triplicate. The error bars indicate standard deviation.

A

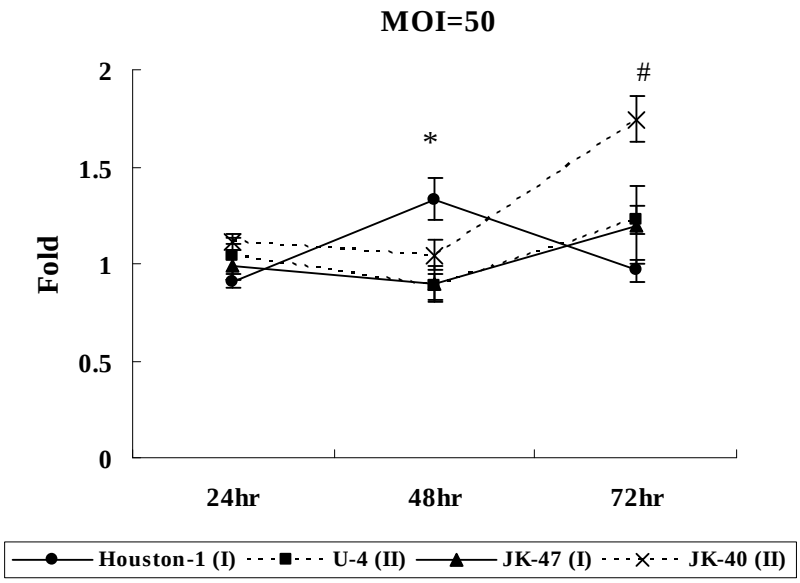

B

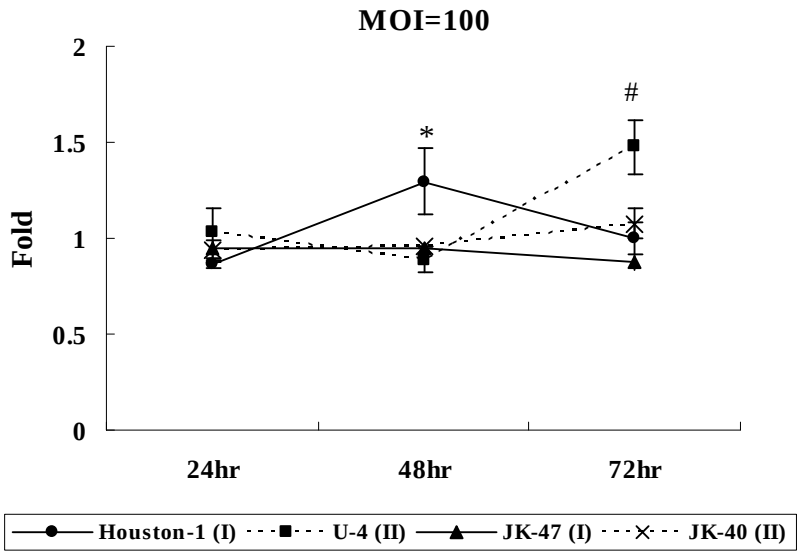

Fig. 1. Effects of *B. henselae* strains on stimulation of HMEC-1 cell proliferation. (A) MOI=50; (B) MOI=100. The numbers in parentheses indicate the 16S rRNA genotype. Results are presented as the mean of the relative fold change as compared with the control groups. *: significant difference (p<0.05) between strains at 48 h; #: significant difference (p<0.05) between strains at 72 h. The results are representative of three independent experiments carried out in triplicate. The error bars indicate

1 standard deviation.

A

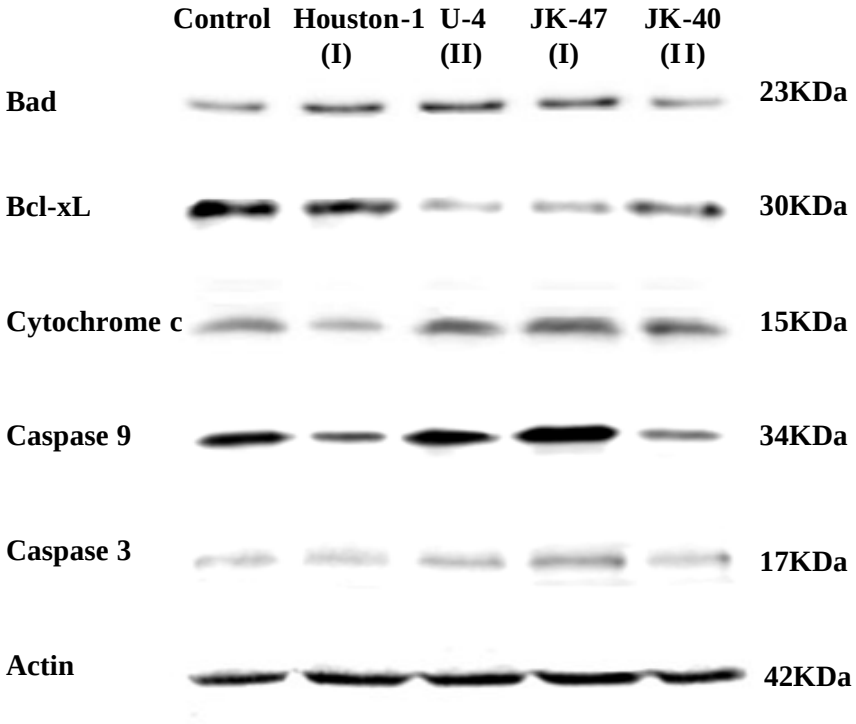

B

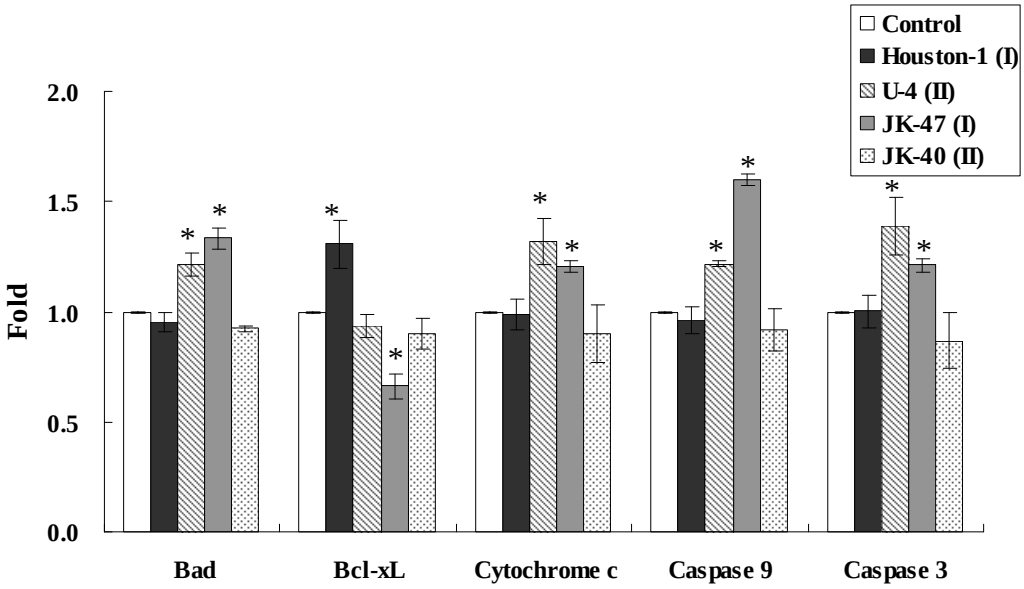

Fig. 2. Effect of *B. henselae* infection on the expression levels of Bad, Bcl-xl, cytochrome *c*, caspase 9 and caspase 3. *: significant difference (p<0.05) in comparison with the control groups (uninfected cells). (A) Western blot; (B) quantitative analysis of Western blot. The numbers in parentheses indicate the 16S

rRNA genotype. All assays were replicated in three independent experiments. The error bars indicate standard deviation.

A

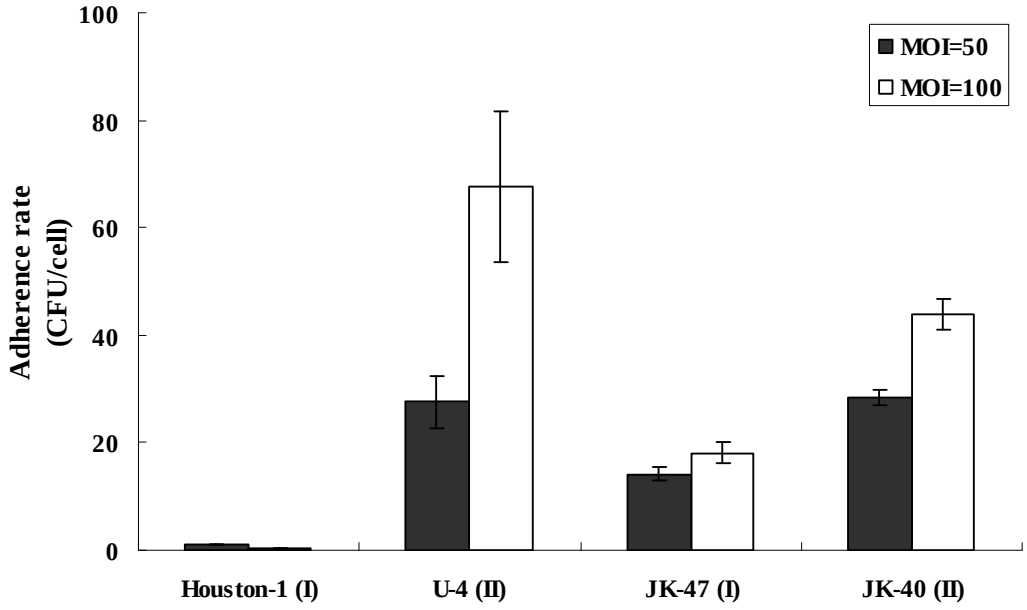

B

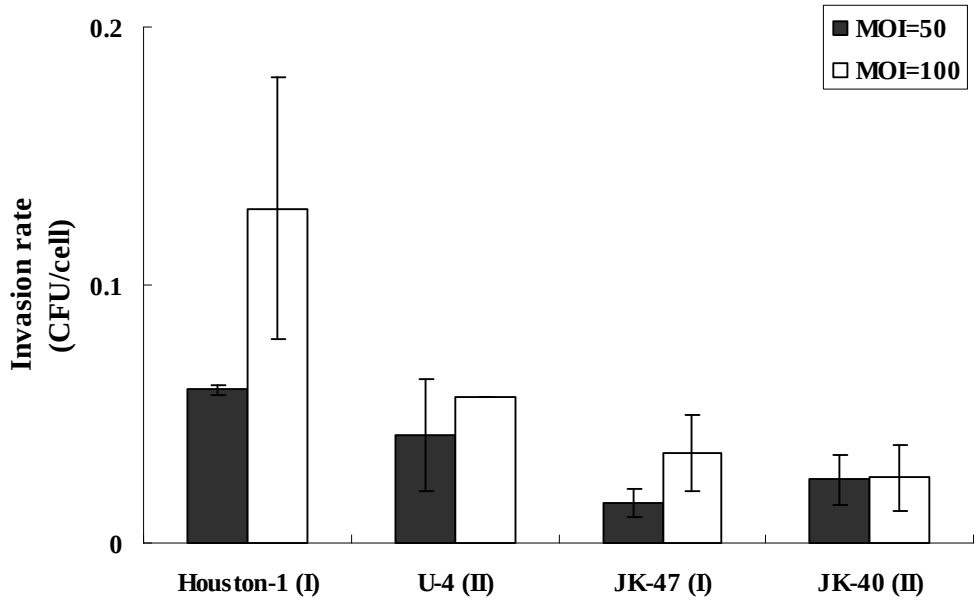

Fig. 3. Association abilities of the different *B. henselae* strains at MOIs of 50 and 100 after 48 and 72 h. (A) adherence rate; (B) invasion rate. The adherence/invasion rates were estimated by dividing the number of adhered/invaded bacteria by the number of HMEC-1 cells. The numbers in parentheses indicate the 16S rRNA genotype. All assays were replicated in three independent experiments. The error bars indicate

standard deviation.

A

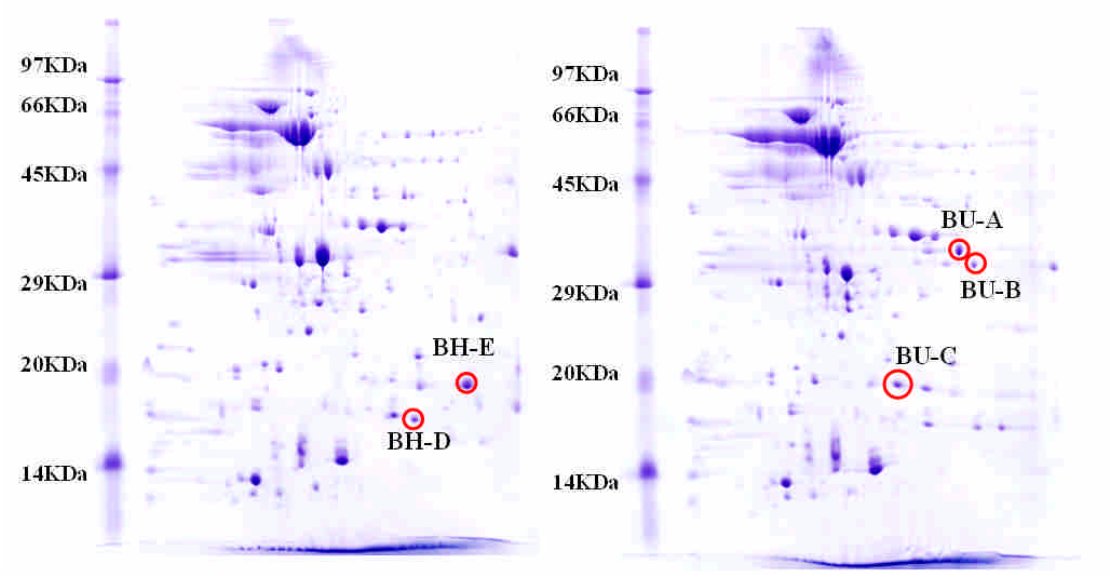

B

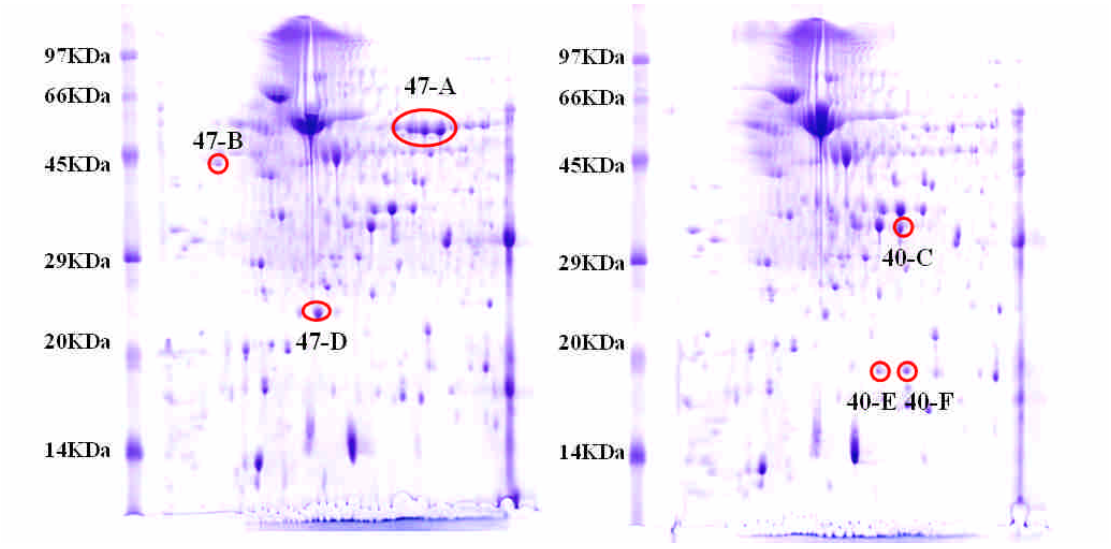

Fig. 4. 2-DE analysis of total proteins in (A) Houston-1 (16S rRNA genotype I, left) and U4 (16S rRNA genotype II, right); (B) JK47 (16S rRNA genotype I, left) and JK40 (16S rRNA genotype II, right).

A

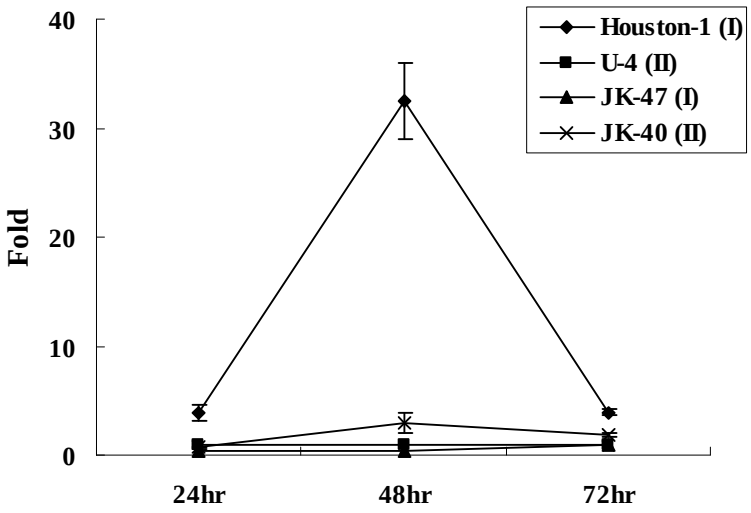
Houston-1 (I)
U-4 (II)
JK-47 (I)
JK-40 (II)
Fold
40
30
20
10
0
24hr
48hr
72hr

B

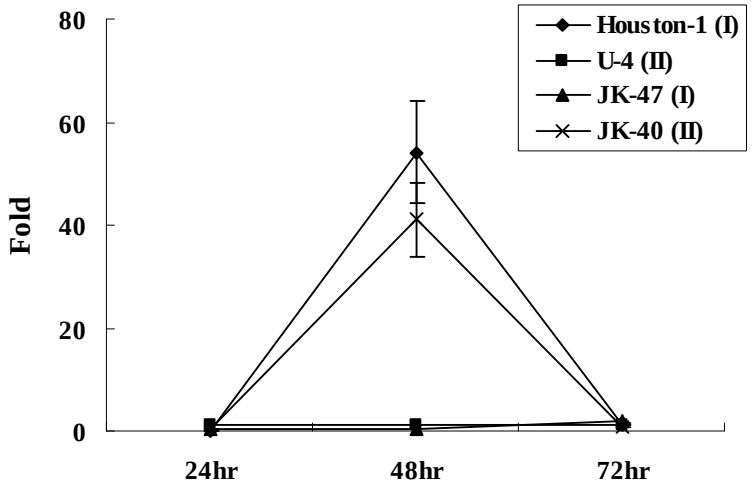
Houston-1 (I)
U-4 (II)
JK-47 (I)
JK-40 (II)
Fold
80
60
40
20
0
24hr
48hr
72hr

C

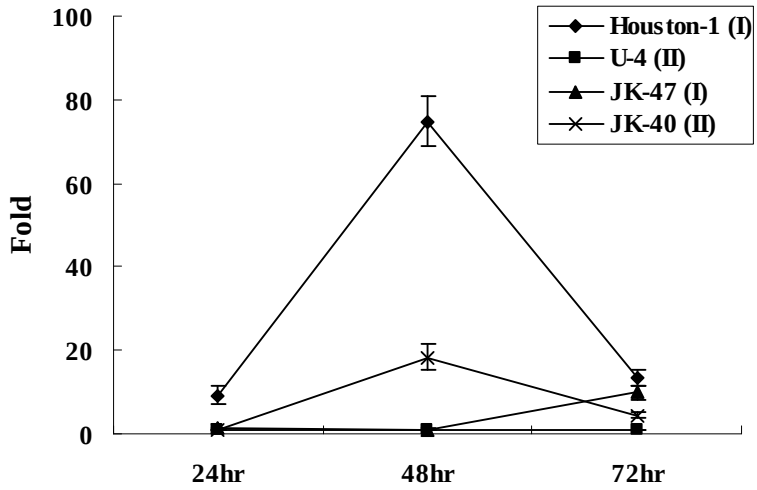
Houston-1 (I)
U-4 (II)
JK-47 (I)
JK-40 (II)
Fold
100
80
60
40
20
0
24hr
48hr
72hr

D

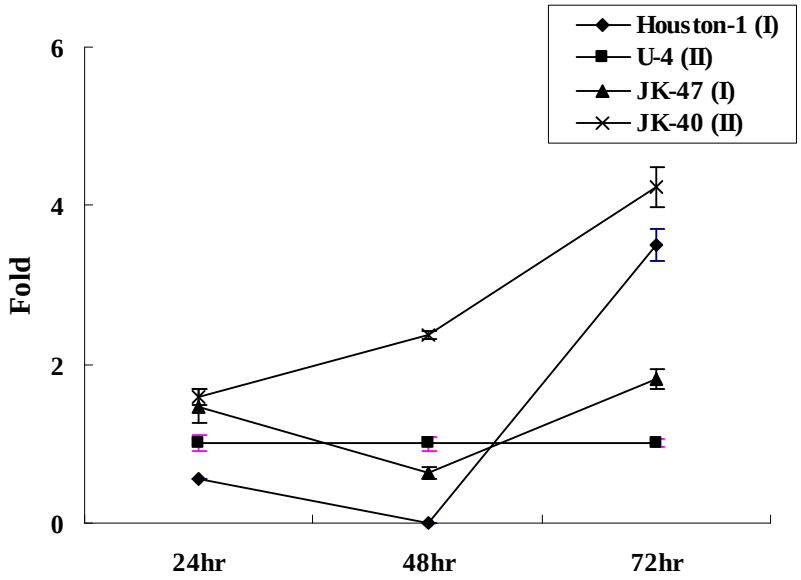
Houston-1 (I)
U-4 (II)
JK-47 (I)
JK-40 (II)
Fold
6
4
2
0
24hr
48hr
72hr

E

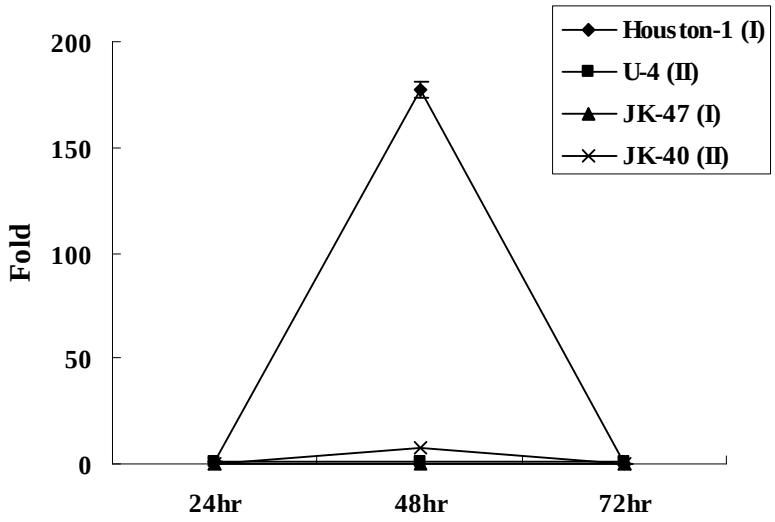

Fig. 5. RNA expression levels of strain-specific proteins in different *B. henselae* strains after infection. (A) BH-D (superoxide dismutase [Cu-Zn] precursor); (B) BU-A (acetyl-CoA carboxylase carboxyltransferase subunit alpha); (C) BU-B (phage-related protein); (D) 47-A (ATP synthase subunit alpha); (E) 40-E (small heat-shock protein). Results are presented as relative fold in comparison with the U-4-infected groups. The numbers in parentheses indicate the 16S rRNA genotype. The results are representative of three independent experiments carried out in triplicate. The error bars indicate standard deviation.